Analysis of Integrity of Surface of Hardened Chromium-Nickel Steel after Finishing Grinding

Dana Stancekova[1], Michal Šajgalík[1], Jozef Mrázik[1], Anna Rudawska[2], Miroslav Janota[1],
[1]University of Zilina, Faculty of Mechanical Engineering, Univerzitna 1, 010 26, Zilina, Slovak Republic, dana.stancekova@fstroj.uniza.sk, pavol.martikan@fstroj.uniza.sk,
[2]Lublin University of Technology, Faculty of Mechanical Engineering, Nadbystrzycka 36, 20-618 Lublin, Poland, a.rudawska@pollub.pl

The paper is focused on the surface integrity in grinding of chromium-nickel steels. These steels are high alloy with an austenitic structure, which guarantees corrosion resistance in combination with high toughness and strength. They are used in various areas. The variety of their use also requires good properties in terms of technical processing. Most high-alloy chromium-nickel steels are well weldable and moldable, but their machinability is a problem, which was also experimentally monitored in the fine grinding process.

Keywords: Chromium-nickel steels, Grinding, Diffractometry

1 Introduction

The submitted paper deals with the issue of grinding of chromium-nickel steel, namely cold hardened chromium-nickel steel. An evaluation of performed experimental verifications is based on a surface integrity, measurement of surface roughness, surface microhardness and residual stress.

Austenitic chromium-nickel cold hardened steel

Steels represent one of the most frequently applied construction materials these days, especially thanks to their fine strength characteristics in proportion to their cost. At the same time, we speak of a very variable material, as by a choice of suitable alloying elements we are able to modify its structure and, thus we may affect mechanical, chemical and physical properties. [1,2]

Non-stabilized chromium-nickel austenitic steels possess relatively low slippage and strength, however, they possess fine plastic properties. The properties predetermine steels to be a suitable material for cold working. As Kuzičin states [3], as a result of cold working there also occurs an increase in strength and slippage and a reduction in ductility.

Machinability of chromium-nickel steels

From the standpoint of machinability, we classify high-alloy chromium-nickel steel as hardly machinable materials. As the company Sandvik Coromant [4] assumes, relative machinability of anticorrosive austenitic steels is about 60%. Worse machinability, at the level of around 30 %, is measured in duplex or super-austenitic steels. The basic reason of reduced machinability of the steels is an origin of high temperatures and forces in the zone of cutting. Among others, it is caused by their physical properties, especially low thermal conductivity. That results in above-mentioned high temperatures in the zone of cutting. [5-7].

Another problems that we face in machining of high-alloy chromium-nickel steel is hardening of a surface layer by a friction of a tool with a machined surface together with a formation of scab on a tool in a set period of cutting speeds.

2 The analysed material is austenite chromium-nickel steel with the label 1.4571 (316Ti).

Firstly, an analysis of structures of samples was performed and then we started to examine a process of grinding. We paid our attention to properties, as we dealt with a titanium-stabilized, molybdenum-alloyed austenitic chromium-nickel steel. Its main component was austenite and it is described by the following characteristics:

- interstitial solid solution of carbon in γ-iron (atoms of an additional component are inserted into the space of a crystal lattice among atoms of basic materials. However, it is possible only in case that atoms of an additional elements are markedly smaller than atoms of a basic material),
- crystals of austenite have light (light grey) colour under a microscope,
- soft, resilient, ductile and nonmagnetic,
- in carbon and low-alloy steels it occurs only in high temperature,
- in high-alloy steel (alloyed by nickel and manganese), austenite remains also in common temperatures.

An original material was machined into a required shape and profile by cold rolling. A sample was taken from the semiproduct. The structure analysis followed. (fig. 1.)

Fig. 1 *Structure of steel 1.4571 (316Ti) after cold rolling*

Material hardening

The given material with its thickness of 8 mm and width 40 mm is used in production in a transformed state. It is machined by cold forming [8]. In our case it is roll bended by the roll bending machine by the company THOMANN (fig. 2 and 3) between rollers to form an O-shape of the product. In this process the material obtains specific properties that affect further machining as well as grinding on a large scale.

Fig. 2 *Material inserted between rollers prepared for bending*

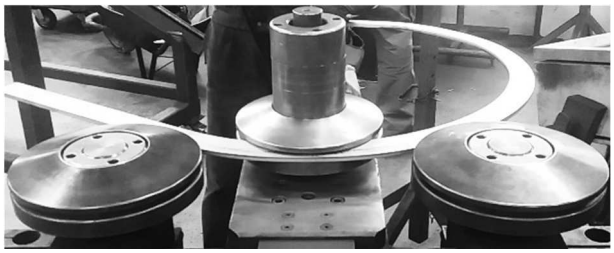

Fig. 3 *Material being bent between rollers into an O-shape product (a flange)*

Material after hardening

Flanges were cut into samples after bending. The samples were analysed and experimental verifications in a process of grinding took place. Even these samples were cut into smaller units for a structural analysis. Fig. 4.a shows the structure in the sample from the outer circumference of bent flanges. It is possible to observe visible enlargements of austenite grains. The enlargement is caused by bending of the material as it is an outer side of a curve of the bent sample.

Fig. 4.b shows a structure in the sample from the inner circumference of bent flanges. It is visible that austenite grains diminished. This was due to compressive forces as it is an inner side of a curve of the bent sample.

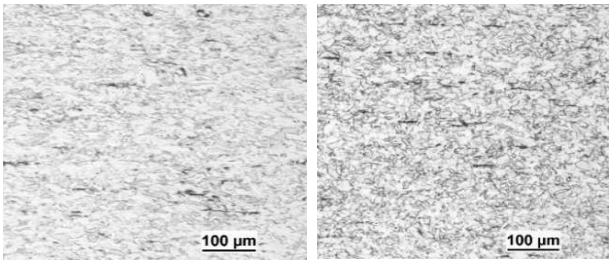

Fig. 4 *Structure of a bent sample in a) outer b) inner circumference*

3 Sample grinding

In experimental verifications we used the grinding machine BPH 21 NA [9], fig. 5, together with a standard oxide grinding wheel from Aluminium Oxide - Al_2O_3 with marked 98A60K9V (200x20x32) mm,

Recommendations for cutting parameters:

- n = 2440 min^{-1} - spindle speed,
- v_c = 25.54 m.s^{-1} - cutting speed of the cutting wheel
- a_p = 0.02 mm x 10 - axial depth of cut,
- f = 5; 10; 15 m.min^{-1} - feed,
- emulsion

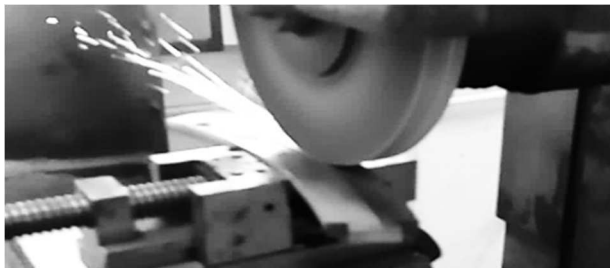

Fig. 5 *Grinding process*

Surface roughness after grinding

Roughness of surface after grinding is one of basic evaluated parameters of integrity of surface. The surftest Mitutoyo SJ-400 (fig. 6 and 7) was used for measurement.

Fig. 6 *Process of roughness measurement*

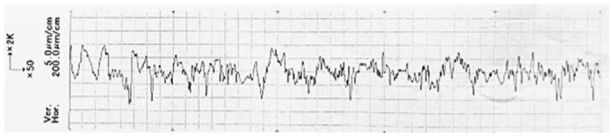

Fig. 7 *Recording of measurement of roughness on the sample*

Measurements were taken on each ground sample on the outer and inner circumference. We expected different values of roughness after grinding.

Measured values

Only selected parameters of surface roughness were evaluated, they are defined by the standard STN EN ISO 4287:

- *Ra* - arithmetical mean roughness value,
- *Rz* - mean roughness depth,
- *Rt* - total height of the roughness profile. [10]

Tab. 1. *An average of measured values of roughness*

Average values in µm				Cutting parameters n = 2440 min^{-1} v_c = 25.5m.s^{-1}
Measurement	Ra	Rz	Rt	
Outer circumference (1)	1.30	8.40	11.27	f = 5 m.min^{-1}
Inner circumference (2)	1.10	6.70	9.17	a_p = 0.2 mm
Outer circumference (3)	1.67	8.84	11.40	f = 10 m.min^{-1}
Inner circumference (4)	0.67	4.80	6.70	a_p = 0.2 mm
Outer circumference (5)	1.13	7.87	10.20	f = 20 m.min^{-1}
Inner circumference (6)	1.39	8.97	10.83	a_p = 0.2 mm

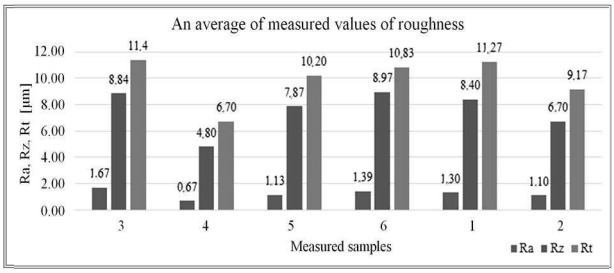

Fig. 8 *Average values of measured parameters of roughness*

Evaluation of surface roughness:

After averaging of measured values, there were obvious differences in measured values of roughness using different grinding parameters.

The most favourable parameter values of roughness *Ra, Rz, Rt* on the surface of verified samples were obtained when applied the following grinding parameters:

- in the inner circumference - feed $f = 10$ m.min^{-1} and depth of cut $a_p = 10$ x 0.2 mm (4),
- in the outer circumference - feed $f = 20$ m.min^{-1} and depth of cut $a_p = 10$ x 0.2 mm (5).
- As it is shown in tab. 1 and the graph in fig.8., measured values of roughness were partially lower in the inner circumference as on the outer circumference of the flange. The differences were due to a change of the structure and residual stress in the material and they were caused by bending (compressional stress in the inner circumference and tensional stress in the outer circumference) and, at the same time, strengthening of the inner part of the curve may take place.

After evaluation, the most suitable parameters of grinding are as follow:

- n = 2440 min^{-1}; v_c =25,54 m.s^{-1}; f = 10 m.min^{-1}; a_p = 10 x 0.2 mm

4 Residual stresses

X-ray diffractometry is applied for measurement of residual stresses that act on the structure of polycrystalline material and on distances of crystal planes. Unless there is no residual stress present, distances of crystallic planes are defined by material properties. The distances may change by an application of residual stress.

The principle of the method is in a measurement of crystal lattice depending on elastic deformation and an application of diffraction of radiation. This method records only a deformation that is adequate to an amount of residual stress. This method i s used together with the instrument Proto iXRD which can be applied to measure residual stress by means of a mounted detector. [10,11]

Material is permanently deformed in case of an application of external forces in machining processes. Against deformation, there act inner forces that are predetermined by structural elements and their mutual interaction (a crystal structure of material).

Tension taking place in the material, after a removal of all external forces acting on a material deformation, is defined as a residual stress in the material. This stress originates under a machined surface only when a plastic deformation of the surface occurs. An origin and all parameters of residual stresses acting in surface layers of a component are directly connected with selected technologies applied during its production. Actions and a nature of residual stresses in surface layers of a machined component results in a significant impact on quality of a machined surface, a decrease of corrosion resistance, an origin of cracks and, last but not least, affecting functionality and overall endurance. [11-13]

Fig. 9 *Point of light showing the X-ray place*

Results of measurements

A final residual stress is an integral value measured at different angles of a mounted detector. A shear or tangentional stress was stated under the term ShearStress. [11]

In Table there are stated values of a normal stress on the surface and just below it. They are measured by means of X-ray diffractometry.

Tab. 2 *Values measured by X-ray diffractometry*

	number	Normal stresses			ShearStress			
Unbent sample		-595.5	±	13.2	-23.0	±	6.8	initial state
bent sample	1	516.4	±	15.0	-36.0	±	7.6	outer curve
	2	296.0	±	18.4	-30.4	±	9.4	
	3	-136.3	±	11.2	-19.9	±	5.7	
	4	-623.5	±	34.4	30.1	±	17.6	
	5	-759.1	±	11.6	-7.3	±	5.9	inner curve
ground sample		-688.6	±	15.1	-20.2	±	7.7	unground surface
	1	1037.5	±	30.7	-80.9	±	15.7	outer curve
	2	958.2	±	23.6	-83.0	±	12.1	
	3	915.5	±	29.8	-79.2	±	19.3	
	4	897.0	±	25.3	-73.6	±	12.9	
	5	914.6	±	29.2	-78.8	±	14.9	
	6	942.8	±	32.9	-84.0	±	16.8	inner curve

In the unbent and unground sample there were measured compressive stresses of the value of 595.5 ± 13.2 MPa. This was due to a fact that an initial material was rolled up to the final state. This process left behind residual stresses in the material. In Table 2 the value is stated with a negative sign (-). That sets the direction of the

given stress. A negative sign defines stress as *compressive* and a positive sign defines stress as *tensional*.

In the process of bending stresses were expected to be tensional in the outer curve, as material is bent along the curve and compressive stresses were expected in the inner curve, as the material is compressed. Several measurements were preformed on a bent but unground sample, a bent and ground sample and in a direction from an outer curve perpendicular even up to the inner curve of the sample.

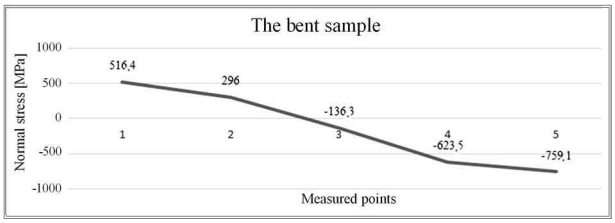

Fig. 10 *Residual stresses in the graph, measured in the bent sample*

5 measurements of residual stresses were performed in the unground sample. As it is shown in Fig. 10, a measured value of a stress in point 1 (516.4±15 MPa) defined a tensional stress in this point which was in accordance with our hypothesis and, thus, that in a given area there occurred a tensional stress as a result of bending. Even in point 2 (296 ± 18.4 MPa) we recorded a value equivalent to a tensional stress.

By further measurement we reached the area in which a structure was compressed. The value measured in the point 3(-136.3 ± 11.2 MPa) defined a compressive stress in this point. This stress condition of compression increases in a direction to the inner side of the curve which was confirmed by values of residual stresses measured in point 4 (-623.5 ± 34.4 MPa) and in point 5 (-759.1 ± 11.6 MPa).

Maximum compressive stresses (-759.1 ± 11.6 MPa) and tensional stresses (516.4±15 MPa) were compared with a value of the elastic modulus by the company of the initial material [-759.1 ± 11.6 MPa << 193 MPa >> 516.4 ± 15 MPa]. The measured values of stresses were much lower than the value of the elastic modulus. This observation confirmed a fact that stresses originating by bending of the initial material do not exceed a maximum value of the elastic modulus. That means that stresses took place in a safe zone.

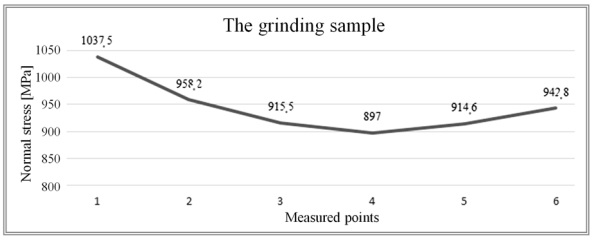

Fig. 11 *Residual stresses in the graph measured in the ground sample*

6 measurements were performed on the ground sample. Values of residual stresses were modified as a result of grinding on the bent sample compared to stresses measured in the unground bent sample. From measured values results that tensional residual stresses took place. As it is shown in Fig. 11 all measured values were positive. That means there were tensional residual stresses. In the outer curve the highest value of a tensional stress was recorded. Even tensional stresses caused by grinding were added to tensional stresses inserted into the material caused by bending.

A maximum measured value of a tensional stress was compared with the value of the elastic modulus of the initial material [1037.5 ± 30.7 MPa << 193 GPa]. Our measured values of residual stresses were much lower than the elastic modulus of the material. That means we are in a safe zone.

To extend the analysis of integrity of surface after grinding, we performed several grindings in which we changed grinding parameters. They were defined in detail in chapter 4.4. After regrinding of samples we measured residual stresses as stated in Tab.3.

Tab. 3 *Values measured by X-ray diffractometry*

sample	normal stresses			shear stresses		
3	1174.5	±	48.3	-26.8	±	25.0
	1162.4	±	47.5	-39.2	±	24.6
4	918.3	±	32.4	-33.0	±	16.8
	1247.5	±	53.3	-38.4	±	27.6
	1209.8	±	46.3	-41.7	±	24.0
5a	1227.9	±	53.1	-31.9	±	27.5
	1248.5	±	52.6	-52.2	±	27.2

As it is shown, a modification of parameters strikingly affected amounts of stresses on the surface of ground samples. In the following chapter we deal with a detailed analysis of measured residual stresses.

Comparison of average values of residual stresses

In this part we compare normal and shear stresses. As we ground bent samples by various grinding parameters, we obtained enough sample surfaces that can be compared regarding a modification of residual stresses before bending, after bending, before grinding and after grinding. As tensional stresses were inserted into a samples surface by grinding, final results are all positive.

Ground samples were compared with the initial material. No post production operation was applied to this sample and that means that the sample was in an original state after rolling. Further samples were bent, but without any surface operations. Here we measured stresses inserted into the material by cold bending. In this operation we had expected that tensional stresses were inserted into the outer side of the curve and compressive stresses into the inner side. Further samples were ground with a modified feed. There were inserted stresses into these samples, namely those originating by grinding. They are tensional stresses. From the above stated facts it is obvious that in points where there were compressional l stresses after bending, there remained tensional stresses after grinding. As stresses inserted into the surface by grinding eliminated stresses inserted by bending and, as a result, in

all ground samples there are measured tensional stresses.

Tab. 4 *Average values of stresses in all samples*

stress [MPa]		normal	shear
unbent sample		-595.5	-23.0
bent sample	outer curve	406.2	-33.2
	inner curve	-691.3	11.4
ground sample	1	918.1	-78.8
	2	970.4	-83.1
	3	1168.4	-33.0
	4	1125.2	-37.7
	5a	1238.2	-42.1

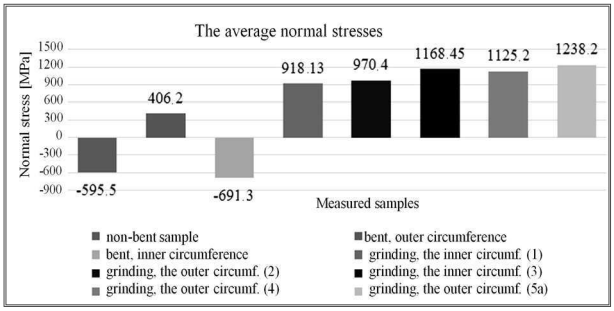

Fig. 12 *Graph containing average normal stresses from all samples*

We compared average values defined from measured values. In samples that were not ground we measured a modification according to the hypothesis, fig. 12. After bending compressive stresses, measured in the initial material, changed. In the outer side of the curve tensional stresses were inserted due to bending. In the inner side of the curve compressive stresses slightly increased. This phenomenon was caused by tension (in the outer curve) of the initial material. By compression (in the inner side of the curve) of the initial material compressive stress increased.

As it is shown in fig. 12, average values of normal stresses are positive in all ground samples, i.e., grinding totally eliminated compressive stresses. In comparison with the initial material, values of stresses were significantly modified.

In ground samples, as shown in fig. 12, parameters of grinding significantly affected residual surface stresses. In comparison with unground samples considerably higher values were measured. By grinding of samples marked 1 and 2, the feed f = 10 m.min^{-1} and depth of the cut a_p = 10 x 0.2 m were applied. Average stresses in the outer and inner curves were measured as positive and that means that grinding left behind tensional stresses in surface layers. In grinding no scales took place.

To grind samples marked as 3 and 4 we modified cutting conditions, namely feed f = 5 m.min^{-1} and depth of the cut a_p = 10 x 0.2 mm. By these cutting conditions we measured increased surface stresses in both sides of the curve. Moreover, scales took place in the outer curve on the surface, fig. 13. This phenomenon negatively affected surface integrity.

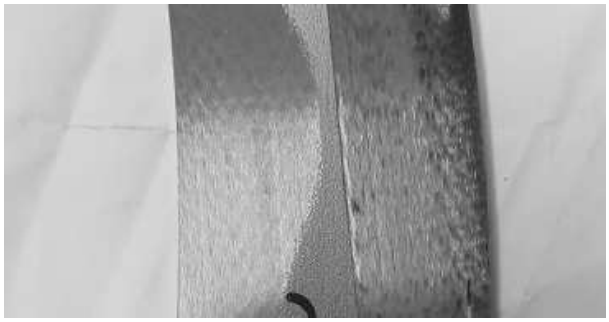

Fig. 13 *Details of ground surfaces 3 and 4*

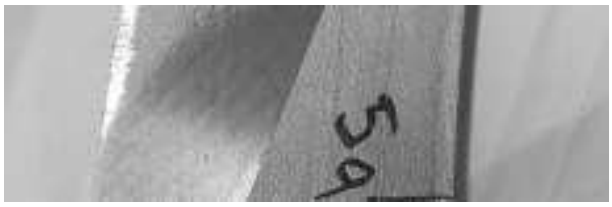

Fig. 14 *Detail of the surface 5a*

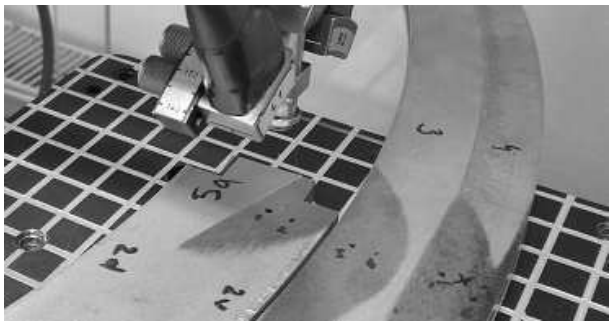

Fig. 15 *Marks of points of measurement of residual stresses.*

Parameters were increased for the last samples marked 5a and 5b compared to the rest, namely the feed f = 20 m.min^{-1} and depth of the cut a_p = 10 x 0.2 m. Residual stresses were measured only in the sample surface marked 5a, as the surface of the sample 5b was placed in the outer side of the curve. An average value of residual stresses measured on the surface was the highest compared to the rest average values. In fig. 15 we see points where residual stresses were measured by red dots. In this sample scales were formed by the above-stated parameters of grinding, as seen in fig. 14. That might partially affect an increase in surface stress. In fig. 14 there are marked points with measured residual stresses.

Cutting parameters of grinding affect final surface stresses. The most favourable residual stresses were measured in surfaces 1 and 2, fig. 12. The grinding parameters n = 2440 min^{-1}; v_c =25.5 m.s^{-1}; f = 10 m.min^{-1}; h = 0.2 mm were the most suitable for grinding of a titanium-stabilized, molybdenum-alloyed austenitic chromium-nickel steel *1.4571 (316Ti).*

5 Conclusion

Experimental verifications were dedicated to address the issue contracted by the company. We deal with machining of a given steel 1.4571. Based on requirements, we completed a structural analysis of the initial material

and the bent material. Here we found out modifications in the structure of the bent material which are specific for this type of forming. Consequently, the bent sample was ground according to set grinding parameters. After grinding, results of an analysis of surface integrity were obtained. Moreover, we provided results of surface roughness measurements after which we selected the most suitable grinding parameters regarding quality of the machined surface. Another measurement was the measurement of parametric integrity of the surface by means of which we obtained values of residual stresses. We measured and compared residual stresses of all samples. After a comparison of stresses of ground and unground samples we selected the most suitable grinding parameters regarding stresses caused by grinding.

From the above-stated results the most suitable grinding parameters of a titanium-stabilized, molybdenum-alloyed austenitic chromium-nickel steel 1.4571 (316Ti) for company conditions are as follow:

- $n = 2440$ min^{-1}
- $v_c = 1532.32$ m.min^{-1}
- $f = 10$ m.min^{-1}
- $a_p = 0.2$ mm measured 10 x

Acknowledgement

The article was made under support grant project KEGA 022ŽU-4/2017 Implementation of on-line education in the area of precise technologies with an impact on educational process to increase skills and flexibility of students of engineering fields of study.

References

[1] NOVOTNÝ, J., LYSONKOVA, I., NAPRSTKOVA, N., MICHNA, S. (2017) Research of application possibilities of selected mechanically alloyed metal powders, In *Manufacturing Technology*, vol. 17, no. 5, p. 811-815.

[2] HRUBÝ, J., RENTKA, J., SCHINDLEROVÁ, V., KREJČÍ, L., ŠEVČÍKOVÁ, X. (2013) Possibilities of prediction of service life of forming tools. In *Manufacturing Technology*, vol. 12, no. 14, p. 178-181.

[3] KUZIČKIN, D., FREMUNT, P., MÍŠEK, B. (1988) *Structural steel, wrought and on castings*. Bratislava: Alfa, 304 p.

[4] SANDVIK COROMANT (2017) *Training Handbook. Metal Cutting Technology.* [Online, 31.1.2018] <http://sandvik.ecbook.se/se/en/training_hand_book/>

[5] VASILKO, K. a kol. (1990). *New materials and technology for their processing*. Bratislava: Alfa, 368 p.

[6] PETRŮ, J., SCHIFFNER, J., ZLÁMAL, T., ČEP, R., KRATOCHVÍL, J., STANČEKOVÁ, D. (2015) Wear Progress of Exchangeable Cutting Inserts During Ti6Al4V Alloy Machining. In *METAL 2015* Conference Procedings of the 24Rd International Conference on Metallurgy and Materials.

[7] HANES, T., HVIZDOŠ, P., ŤAVODOVÁ, M., KALINCOVÁ, D., HRICOVÁ, J., BEŇO, P. (2014) Coating surface roughness measurement made on coining dies. In *Manufacturing technology,* vol. 14, no. 3, p. 309-317.

[8] SAPIETA, M; SAPIETOVA, A; DEKYS, V. (2017) Comparison of the thermoelastic phenomenon expressions in stainless steels during cyclic loading. In. METALURGIJA, vol. 56, Issue: 1-2, 2017, p. 203-206.

[9] NESLUSAN, M., BAMUROVA, J., MICIETOVA, A., CILLIKOVA, M. (2016) Performance of Norton Quantum Grinding Wheels. In *Key Engineering Materials*, Vol. 686, p. 125-130

[10] CEP, R., JANASEK, A., PETRU, J., SADILEK, M., MOHYLA, P., VALICEK, J., HARNICAROVA, M., CZAN, A. Surface Roughness after Machining and Influence of Feed Rate on Process. In *Key Engineering Materials*, Vol. 581, pp. 341-347.

[11] DRBÚL, M., ŠAJGALÍK, M., ŠEMCER, J., CZÁNOVÁ, T., PETRKOVSKÁ, L., ČEPOVÁ, L. (2014) *Engineering Metrology and the quality of surfaces created by machining technologies.* Žilina: ŽU v Žiline, 115s.

[12] ČUBOŇOVÁ, N., KURIC. I. (2014) Data structures implementation of the protocol STEP-NC at CNC machines programming. In: Communications, vol. 16, no. 3A, pp. 176-183.

[13] VALÁŠEK, P., MÜLLER, M. (2015). Abrasive wear in three-phase waste based polymeric particle composites. In. *Tehnicki Vjesnik-Technical Gazette*, vol. 12, 2/2015, pp. 257-262.

10.21062/ujep/186.2018/a/1213-2489/MT/18/5/833